Plasma Science and Technology

PAPER

Research on quinoline degradation in drinking water by a large volume strong ionization dielectric barrier discharge reaction system

To cite this article: Rongjie YI *et al* 2021 *Plasma Sci. Technol.* **23** 085505

View the article online for updates and enhancements.

This content was downloaded from IP address 210.73.19.177 on 02/07/2021 at 01:36

© 2021 Hefei Institutes of Physical Science, Chinese Academy of Sciences and IOP Publishing Printed in China and the UK

Plasma Sci. Technol. **23** (2021) 085505 (15pp) https://doi.org/10.1088/2058-6272/abffa9

Research on quinoline degradation in drinking water by a large volume strong ionization dielectric barrier discharge reaction system

Rongjie YI (依蓉婕), **Chengwu YI** (依成武), **Daolin DU** (杜道林), **Qi ZHANG** (张琪), **Haijun YU** (喻海军) **and Liu YANG** (杨柳)

School of Environment and Safety Engineering, Jiangsu University, Zhenjiang 212013, People's Republic of China

E-mail: 1000003131@ujs.edu.cn and yichengwu0943@163.com

Received 20 January 2021, revised 7 May 2021
Accepted for publication 10 May 2021
Published 30 June 2021

Abstract

Quinoline is widely used in the production of drugs as a highly effective insecticide, and its derivatives can also be used to produce dyes. It has a teratogenic carcinogen to wildlife and humans once entering into the aquatic environment. In this study, the degradation mechanism of quinoline in drinking water by a strong ionization dielectric barrier discharge (DBD) low-temperature plasma with large volume was explored. High concentration of hydroxyl radical (·OH) (0.74 mmol l^{-1}) and ozone (O_3) (58.2 mg l^{-1}) produced by strongly ionized discharge DBD system were quantitatively analyzed based on the results of electron spin resonance and O_3 measurements. The influencing reaction conditions of input voltages, initial pH value, ·OH inhibitors, initial concentration and inorganic ions on the removal efficiency of quinoline were systematically studied. The obtained results showed that the removal efficiency and TOC removal of quinoline achieved 94.8% and 32.2%, degradation kinetic constant was 0.050 min^{-1} at 3.8 kV and in a neutral pH (7.2). The proposed pathways of quinoline were suggested based on identified intermediates as hydroxy pyridine, fumaric acid, oxalic acid, and other small molecular acids by high-performance liquid chromatography/tandem mass spectrometry analysis. Moreover, the toxicity analysis on the intermediates demonstrated that its acute toxicity, bioaccumulation factor and mutagenicity were reduced. The overall findings provided theoretical and experimental basis for the application of a high capacity strong ionization DBD water treatment system in the removal of quinoline from drinking water.

Keywords: dielectric barrier discharge, hydroxyl radical, ozone, quinoline, strong ionization discharge, toxicity

(Some figures may appear in colour only in the online journal)

1. Introduction

Quinoline is a common contaminant widely existing in coking wastewater, dyeing wastewater, pharmaceutical wastewater, and printing wastewater, generally resistant to biodegradation, with the characteristics of carcinogenic, teratogenic and mutagenic [1, 2]. Discharge of untreated quinoline into aquatic can have serious impacts on the aquatic ecosystems, particularly with potential mutagenic threats to wildlife and humans in drinking water sources [3, 4]. Conventional wastewater treatments cannot completely remove these pollutants [5]. Thus, it is very important to completely remove the quinoline from the water body before entering into the aqueous environment [6].

Nowadays, various degradation methods of quinoline have been used, mainly including microorganisms, adsorption media, electrochemical oxidation and advanced oxidation

processes (AOPs). Recent studies investigating the biodegradation after photolysis and the biodegradation have shown that quinoline biodegradation is accelerated by 19% and 50%, respectively, by adding oxalic acid commensurate with the amount produced by photolysis [7]. As described by Qiao *et al* and Lee *et al* quinoline could be effectively degraded by biodegradation, with the disadvantages of a long treatment cycle, low mineralization and high selectivity of special microorganisms [8, 9]. Therefore, various AOPs methods have been proposed to improve the quinoline removal efficiency over the past years. Wang *et al* used a biochemical system-electric Fenton system to deepen the treatment of coal gasification wastewater, confirmed that the co-metabolism of phenol as the first substrate of high-quality carbon denitrification source could improve removal efficiency of quinoline and pyrrole in anoxic conditions [10]. Additionally, Liu *et al* also reported that $CuFe_2O_4$/SEP catalyzed ozonation of quinoline mineralization rate up to 90.3%, $CuFe_2O_4$/SEP catalyzed ozonation of quinoline mineralization rate constant 16.7 times that of O_3 alone [2]. However, while improving the removal efficiency and mineralization rate, the AOPs process still has some shortcomings, such as the addition of catalyst increases the treatment cost, and the recovery of catalyst is also an important task. Meanwhile, the core issues of AOPs were the low yield and low concentration of hydroxyl (·OH), transformation products were complicated, which were only applied to a small-scale application [11–13]. Thus, to overcome these shortcomings in water treatment, a new method of AOPs which can produce high yield and high concentration ·OH without adding any catalyst has been paid more attention.

Dielectric barrier discharge (DBD) low-temperature plasma technology can overcome the aforementioned issues. Several attempts by DBD to degrade organic pollutants from aqueous solutions have shown that conventional DBD can effectively and non-selectively remove pollutants in a short period of time [14–16]. However, certain deficiencies restricted the broad application of the traditional DBD, Wang *et al* studied the degradation of methylene blue in 50 ml aqueous solution by a DBD system [17]. The treatment capacity of DBD system studied by Iervolino *et al* was only 0.09 l min^{-1} [18]. Guo *et al* investigated the degradation of ofloxacin in water by plasma coupled with graphene-Fe_3O_4 nanocomposites, the capacity of the treatment water is only 150 ml [19]. Other studies have also confirmed that the traditional DBD has a lower treatment capacity to the laboratory level. None of the reaction systems can be used on a large scale [20–23]. Moreover, high power demand and mass transfer of low-reactive substances from plasma to the aqueous medium are also disadvantages of the traditional DBD systems [18, 22, 23].

Hence, based on the low temperature plasma theory of strong ionization discharge, a strong ionization DBD reaction system for degrading quinoline in water was developed in this study. The strong ionization discharge method can overcome the shortcomings, which can produce high electron concentration ($>10^{15}$ cm^{-3}) and large electron energy (>10 eV), to ionize H_2O molecules and O_2 molecules in a short time for producing a lot of free radicals, such as high concentration ·OH, and O_3, which can oxidize and degrade contaminant [14, 24, 25]. This strong ionization discharge DBD system has the advantages of short reaction time, high removal efficiency, low cost, low energy consumption and smaller footprint through improvements of plate gap, discharge medium and other structure and process parameters. Moreover, the strong ionization discharge DBD sewage treatment volume was 40 l, and the water flow was 33.3 l min^{-1}, for large-scale industrial treatment of sudden environmental pollution drinking water. Another advantage of this research is the introduction of Venturi jets, the principle of combined jets can improve the mass transfer of active particles from plasma to aqueous solution medium and greatly increase the number of active particles. Furthermore, it is worth stressing that the intermediate by-products were more toxic than original compounds. Therefore, it is more important to study the toxicity evaluation of quinoline and its intermediate byproducts.

In this work, the sewage treatment volume of the system was increased to 40 l, which is much higher than the existing DBD water treatment system. By combining with the Venturi tube, the number of active particles (·OH and O_3) in the water is increased. Hence, a new method for the removal of quinoline by a large volume strong ionization discharge DBD was proposed. Therefore, the objectives were: (1) to quantify the existence of high concentration of ·OH and O_3 produced by a strong ionization DBD in the system; (2) to assess the effect of applied voltages, initial concentration, ·OH inhibitor, inorganic matter and initial pH values on quinoline removal by a new plate-type strong ionization DBD; (3) to identify the transformation by-products and propose a possible degradation pathway of quinoline under a strong ionization DBD process; (4) to evaluate the toxicity of intermediate by-products by Toxicity Estimation Software Tool (TEST, version 4.2.1). This study can provide a valuable reference for the efficient treatment of quinoline in contaminated water.

2. Material and methods

2.1. Experimental apparatus

The process diagram of the strong ionization DBD low-temperature plasma water treatment system was shown in figure 1. The water treatment system was mainly composed of a strong ionization discharge DBD generator, 33.3 l min^{-1} water circulation system, instrument control and monitoring system, high-frequency and high-voltage power supply. AC power supply can convert 220 V/50 Hz power frequency to 0–4.5 kV/0–60 kHz high-frequency voltage. The water circulation system mainly included water circulation pump, Venturi jet, gas–liquid mixing device, gas–liquid separator, rotor flowmeter, pipeline, etc. The active particles produced by a strong ionization discharge generator entered the water through the Venturi jet device and underwent a thorough mixing reaction in the gas–liquid dissolution device. Then, the reaction liquid entered the gas–liquid separation device to separate the unreacted O_3 or O_2 from the reaction solution and

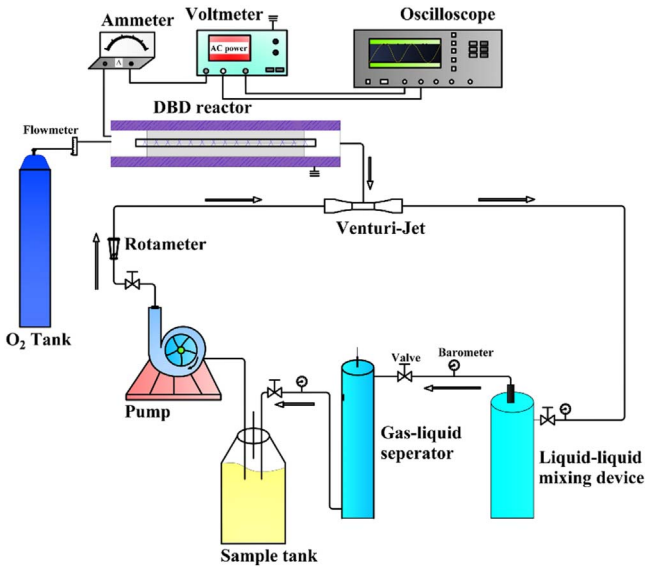

Figure 1. The flow-process diagram of water treatment systems of strong ionization dielectric barrier discharge.

returned to the sample barrel for recycling under the action of the circulating pump, and the residual gas was emptied through the pipeline.

Figure 2 depicted the working mechanism of a discharge generator with a strong ionization dielectric barrier. The structure of the DBD generator consisted of grounding electrode, electrical insulator, discharge electrode (silver), the ceramic dielectric layer (α-Al_2O_3) and heat sink. The plate size of the grounding electrode and discharge electrode were 40 cm × 20 cm × 1 cm and 40 cm × 20 cm × 1 mm, respectively. The discharge electrodes were made of the material metallic silver, and coated with a thin (330 μm) dielectric layer composed of dense insulating α-Al_2O_3 powder, and the stainless steel case was the grounding electrode. The electrical insulator was placed between the discharge plate and the grounding electrode to keep plate clearance between 0.2 mm. When O_2 molecules collide through the discharge gap (0.1–1 mm) under the action of the external electric field discharge point, O_2 electron avalanche will occur and a large number of microfilamentous pulse discharge would be formed. At this time, the E/N equivalent electron strength exceeds 500×10^{-17} V · cm^2, which meets the condition that oxygen and water molecules could be directly ionized into high concentration hydroxyl at the molecular level [14, 24]. The discharge intensity of the electric field (E_g) and electronic energy (T_e) in the discharge gap can be expressed by the following formulas [25]:

$$E_g = \frac{V\varepsilon_d}{2L_d\varepsilon_g + L_g\varepsilon_d} \tag{1}$$

$$T_e = \frac{\sigma m_h {E_g}^2}{3kn_e m_e {v_e}'}, \tag{2}$$

where, E_g (kV cm^{-1}) refers to electric field intensity, and L_g (cm), L_d (cm), ε_g are the thickness of plate clearance or medium and permittivity, respectively. T_e represents electronic energy, and m_h(eV), m_e(eV) and n_e(cm^{-3}) are the mass of electronic and heavy particles and electron concentration, respectively. σ (μS cm^{-1}), k and ${v_e}'$ (s^{-1}) stand for plasma conductivity, Boltzmann constant and electron collision frequency, respectively. Due to the selection of discharge electrode (silver) and ceramic dielectric material (α-Al_2O_3 > 99.5%, dielectric constant 8.1) and the setting of discharge gap (0.64 mm), the excitation frequency was more than 6 kHz, the excitation voltage was 3.8 kV, the maximum electric field intensity was as high as 800 kV cm^{-1}, the electron density was as high as 10^{15} cm^{-3}, the discharge energy density of plate gap was 2.1 W cm^{-2}, and the average electron energy increased from 10 eV to more than 13 eV [14]. Strong ionization discharge intensity (E_g), electron concentration (E_n), electron energy (T_e) and discharge electric field intensity (I) were much higher than those for other traditional DBDs, as shown in table 1, which can produce uniform and stable streamer discharge compared with other discharge methods [26–28]. Thus, compared with ordinary micro discharges, strong ionization discharge can ionize O_2 more easily and produce more active free radicals. Meanwhile, super excited state, ionization and dissociation occur in the oxygen reaction in the discharge gap (R1–R5), resulting in O_3, O^+, O_2^+, O_2^-, etc [29].

$$O_2 + e \rightarrow O^+ + \cdot O + 2e \tag{R1}$$

$$O_2 + \cdot O \rightarrow O_3 \tag{R2}$$

$$O_2 + e \rightarrow O_2^+ + 2e \tag{R3}$$

$$O_2 + e \rightarrow O_2^- \tag{R4}$$

$$O_2^+ + O_2^- \rightarrow O_3 + \cdot O. \tag{R5}$$

Additionally, a Venturi jet was added in the circulation system. Through the principle of jet, a large amount of O_3 and a little oxygen free radicals (O^+, O_2^+, O_2^-, etc) combining with H_2O to form ·OH, ·HO_2, etc, the generated active particles were injected into the water circulation system. ·OH and active particles were produced through the following routes (R6)–(R9):

$$O_2^+ + H_2O + M \rightarrow O_2^+(H_2O) + M \tag{R6}$$

$$O_2^+(H_2O) + H_2O \rightarrow H_3O^+ + O_2 + \cdot OH \tag{R7}$$

$$O_2^+(H_2O) + H_2O \rightarrow H_3O^+(\cdot OH) + O_2 \tag{R8}$$

$$H_3O^+(\cdot OH) + H_2O \rightarrow H_3O^+ + O_2 + \cdot OH. \tag{R9}$$

Under the condition of strong ionization discharge, the existence of O_2 provides raw material guarantee for the formation of active particles (O_3, O^+, O_2^+, O_2^-, etc). The form of generated plasma in this study was strong ionization discharge, with a higher electron energy of 13 eV, a higher electric field strength of 800×10^{-17} V · cm^2 and a higher electron density of 10^{15} cm^{-3}, which can improve the energy guarantee for the production of high concentration of ·OH, O_3 and other active particles. Meanwhile, the combination with the Venturi jet had a positive effect on mixing to generate a large number of ·OH and other active particles (·HO_2, H_3O^+, etc) with stronger oxidation ability. Thus, quinoline and its intermediates by-products in water can be effectively removed by strong ionization discharge low-temperature plasma water treatment system.

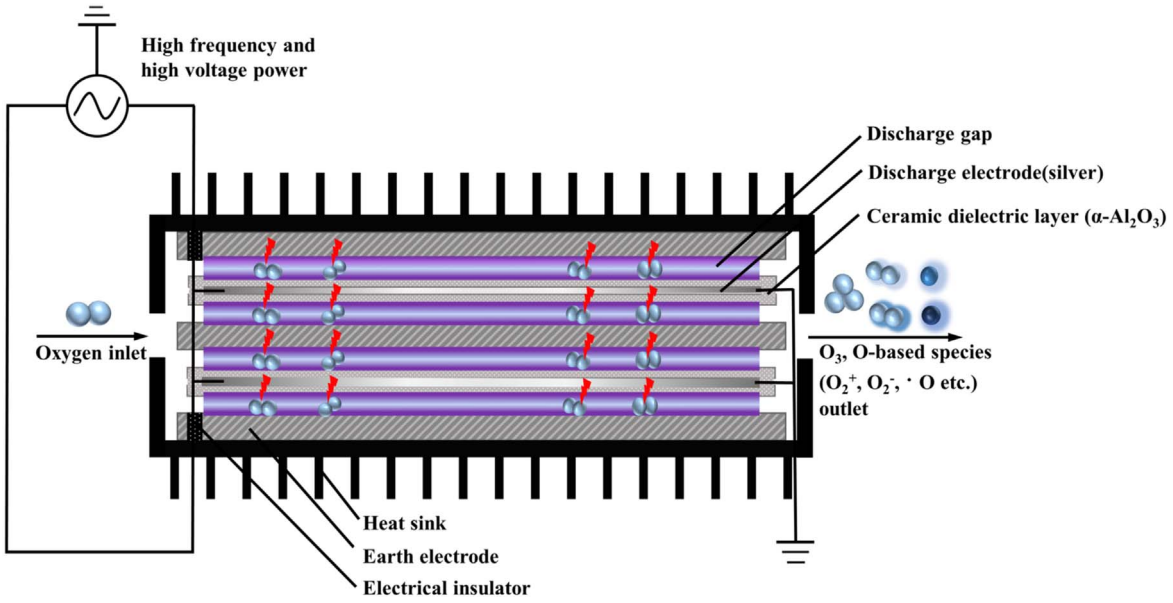

Figure 2. Schematic diagram of a strong ionization discharge DBD reactor.

2.2. Experimental materials

Quinoline (99%), *tert*-butanol (TBA), formic acid, 5,5-dimethyl-1-pyrrolidine N-oxide (DMPO, 97%), oxalic acid and methanol were obtained at analytical grade, purchased from Sigma-Aldrich (USA). Formic acid, sodium carbonate was supplied by Aladdin Industrial Corporation Ltd (China). Sodium thiosulfate and sodium bicarbonate were purchased from Chinese National Medicines Corporation Ltd (China).

Table 1. Comparison of discharge parameters between strong ionization discharge and dielectric barrier discharge.

Discharge parameters	Strong ionization discharge	Micro dielectric barrier discharge
Electric field intensity	100–320 kV cm^{-1}	0.1–100 kV cm^{-1}
Electron average energy	>10 eV	1–10 eV
Discharge energy	1–2.1 W cm^{-2}	<1 W cm^{-2}
Electron concentration	$>10^{15}$ cm^{-3}	10^{14}–10^{15} cm^{-3}

2.3. Analytical methods

The concentrations of quinoline in drinking water were measured by a UV–visible spectrophotometer (UV-22450, Shimadzu Corporation, Japan) at 280 nm. The degradation tendency of quinoline and changes of pH value in the reaction process was observed with a TOC survey meter (TOC-VCPH/CPN, Shimadzu Corporation, Japan) and pH meter (FE20, METTLER TOLEDO, China). The intermediate byproducts of degradation of quinoline were diagnosed by a high-performance liquid chromatography/tandem mass spectrometry (LC–MS) (7890B-5977B, Agilent), equipped with a 250 mm × 4.6 mm × 5 μm Waters Xbridge C18 column. Detailed methods of LC–MS can be found in table A1. The concentrations of O_3 generated during the process were measured with a high concentration ultraviolet O_3 gas analyzer (KEN-2000, KEN, USA) and dissolved with a water O_3 analyzer (CL-7685, B&C electzanice, Italy), respectively. Electron spin resonance (ESR) were obtained with a Bruker MicroESR spectrometer (Karlsruhe, Germany). Details for the analysis are presented in table A2. After strong ionization DBD treatment, the intermediate byproducts' toxicity of quinoline was evaluated via the US Environmental Protection Agency Toxicity Estimation Software Tool (T.E.S.T.) based on quantitative structure activity relationships methodologies [30].

The degradation of quinoline efficiency was defined as equation (3):

$$\text{Degradation efficiency}(\%) = \frac{(\text{Quinoline})_0 - (\text{Quinoline})_t}{(\text{Quinoline})_0} \times 100, \quad (3)$$

where, $(\text{Quinoline})_0$ is the quinoline initial concentration (mg l^{-1}), $(\text{Quinoline})_t$ is the quinoline concentration at strong ionization discharge time (mg l^{-1}).

In this experiment, a 40 l quinoline solution with an initial concentration of 20 mg l^{-1} was poured into a mixing tank and stirred evenly. Under the action of the recirculation pump, the water flow reached 33.3 l min^{-1}. Then, O_2 was turned on and the indicator was observed to control it to 5 l min^{-1}. At the same time, according to adjusted parameters of the ammeter and voltmeter and observed changes of the display parameters of the oscilloscope, the optimal power supply parameter range of the strong ionization DBD generator was determined, so that the voltage was maintained in the range of 2.6–4.1 kV, the frequency was 15–23 kHz, and the current was 0.6–1.2 A. After setting the parameters, the outlet of the strongly ionized DBD generator was connected to the Venturi jet. The sewage treatment volume of this experiment was 40 l under the 33.3 l min^{-1} water flow,

and the experiment time was 0 min, 5 min, 10 min, 20 min, 30 min, 45 min and 60 min, respectively. After sampling at the set time (0 min, 5 min, 10 min, 20 min, 30 min, 45 min and 60 min), 50 ml of the same amount of solution was placed in the tube and sodium thiosulfate (0.05 mol l^{-1}) was added immediately to stop the reaction.

3. Results and discussion

3.1. Determination of major reactive species in the reaction process

The existence and the concentration of active species produced by strong ionization DBD are important factors affecting the removal efficiency of organic pollutants. To quantify the number of ·OH in a strong ionization discharge DBD system, an ESR spectrometer was performed with DMPO as the spin-trapping reagent, to test the existence of free radicals in a strong ionization discharge DBD system. As shown in figure 3(a), the 1:2:2:1 quartet signal characteristic of DMPO-·OH adducts appears on the spectrum displayed by ESR. According to the signal in the ESR spectrometer, the concentration of the ·OH increased with the reaction time. Referring to the peak area of ·OH signal in ESR and the calibration curves (figure A1), the ·OH concentration was 0.74 mmol l^{-1}. Meanwhile, the variation of ·OH production at different times was illustrated in figure 3(b), the concentration of ·OH increased within 20 min, and stabilized after reaction time. It was confirmed that a large amount of ·OH existed in a strong ionization discharge DBD system. Based on the theory of strong ionization discharge DBD low-temperature plasma technology, O_3 is also generated in addition to ·OH as the main active substance [15]. In this experiment, the concentration of O_3 water dissolution at the outlet of the DBD system with strong ionization discharge was measured under the voltages of 2.1 kV 2.8 kV, 3.0 kV, 3.3 kV and 3.8 kV, respectively. As illustrated in figure 3(c), with the increase of the input voltage, the O_3 content generated by the strongly ionized DBD system also increases. When the applied voltage reached 3.8 kV at 20 min, the production of O_3 reached 58.2 mg l^{-1} and the dissolved amount in water reached 13.4 mg l^{-1}. Besides, the variation of O_3 concentration at different times was shown in figure 3(d), the trend of O_3 production was consistent with that of water dissolution, the accumulation of O_3 increased with the extension of time. Compared to the other plasma technology, such as pulsed discharge plasma (PDP) coupled with complex catalysis (rGO-WO_3-Fe_3O_4), the concentration of ·OH was 0.172 mmol l^{-1}, 0.201 mmol l^{-1}, 0.243 mmol l^{-1} and 0.269 mmol l^{-1}, respectively (PDP, PDP-WO_3, PDP-rGO-WO_3, PDP-rGO-WO_3-Fe_3O_4) [15], while, the strong ionization discharge DBD system can produce a higher concentration of ·OH (0.74 mmol l^{-1}) and O_3 (13.4 mg l^{-1}) without adding any catalyst and applying for large capacity. Therefore, a large amount of ·OH and O_3 can be produced in the strong ionization

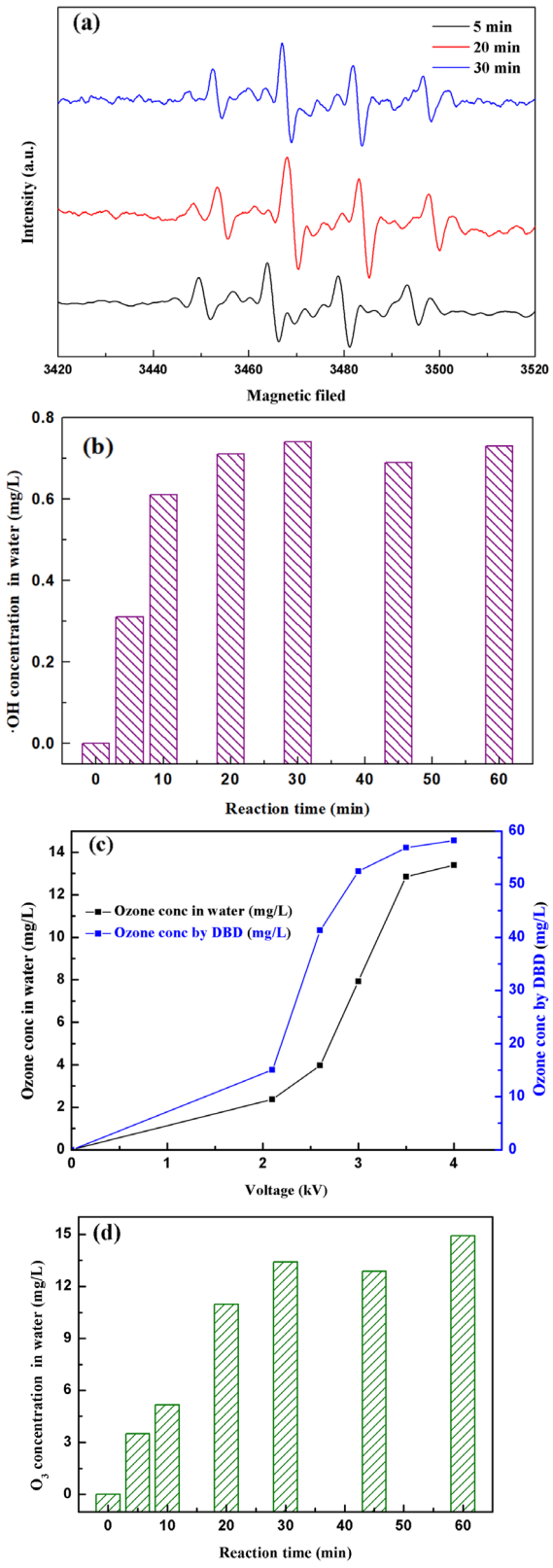

Figure 3. Verification of active particles in strong ionization dielectric barrier discharge reaction system. (a) ESR spectrum, (b) ·OH concentration in water at different times, (c) O_3 concentration in water and in DBD at different times, (d) O_3 concentration in water on different voltages.

discharge DBD system, which can provide a guarantee for removing quinoline more effectively.

3.2. Effects of reaction conditions on degradation of quinoline

3.2.1. Effect of input voltage on degradation of quinoline. The input voltage plays a crucial role in the degradation of quinoline in a strong ionization discharge DBD system by affecting the production of active species. In general, with the increase of the input voltage, the degree of ionization between the plates will be further increased [31]. In order to protect the high-frequency and high-voltage power supply and generator without reducing the production efficiency of active particles, experiments investigated the change of quinoline degradation efficiency in water samples at different voltages (2.8, 3.3 and 3.8 kV), and plotted the curve as shown in figure 4(a). At different input voltages, the removal efficiencies of quinoline were 78.4%, 87.2% and 94.8% after 60 min treatment, respectively. Similarly, figure 4(b) showed that the kinetic constant can be enhanced when the input voltage increased. At the peak voltage of 3.8 kV, the kinetic constant can reach up to 0.050 min^{-1}. As illustrated in figure 3(d), the concentration of O_3 produced also enhanced with the increase of the input voltage. It is clear that increasing the input voltage can lead to the increase of quinoline removal, indicating that the input voltage was an important factor affecting the treatment effect of the strong ionization discharge in the treatment of water pollutants. While, as can be seen from table A3, it is worth emphasizing that the removal efficiency of contaminants increased with the increase of the input voltage, so did energy consumption. As the input voltage increased from 2.6 to 3.8 kV, the energy consumption increased from 0.082 to 0.195 kWh, and quinoline abatement showed a consistent decreasing tendency for all the samples. Nevertheless, compared to existing organic wastewater treatment methods of the sewage treatment plant in table A4, the energy consumption of the wastewater treatment plant with strongly ionized discharge plasma technology requires the lowest energy consumption, which is well below those of the activated sludge process (12 times), contact oxidation process (13 times), chemical oxidation process (10 times) and chemical oxidation process (178 times) methods. Asaithambi *et al* investigated the treatment of leachate wastewater from landfill waste by sonication (US)/O_3/electrocoagulation (EC) process, with the energy consumption of 8 kWh m^{-3} [32]. Meanwhile, the energy consumption of single processes such as O_3 only, US/O_3 and O_3/EC was 13.35 kWh m^{-3}, 30.34 kWh m^{-3} and 7.8 kWh m^{-3}, respectively [33–35]. Irani *et al* used O_3 pre- and post-treatment combined with bio-attached growth reactor to remove ammonia nitrogen from actual urban sewage, with the average energy consumption calculated of 57.43 kWh m^{-3} and 51.41 kWh m^{-3} for pre- and post-ozonation processes, respectively [36]. Therefore, compared with the existing O_3 treatment system, the energy consumption of strong ionization discharge DBD was only 0.133 kWh, which was far lower than that of the existing O_3 technology. Besides, the active substance produced by strong ionization discharge was much higher than that of ordinary O_3 device, with the ·OH content and O_3 content of 0.74 mmol l^{-1} and 58.2 mg l^{-1}, respectively. Therefore, strong ionization discharge system has high pollutant removal efficiency and low operation cost, with good application prospect and economic value in industrial application.

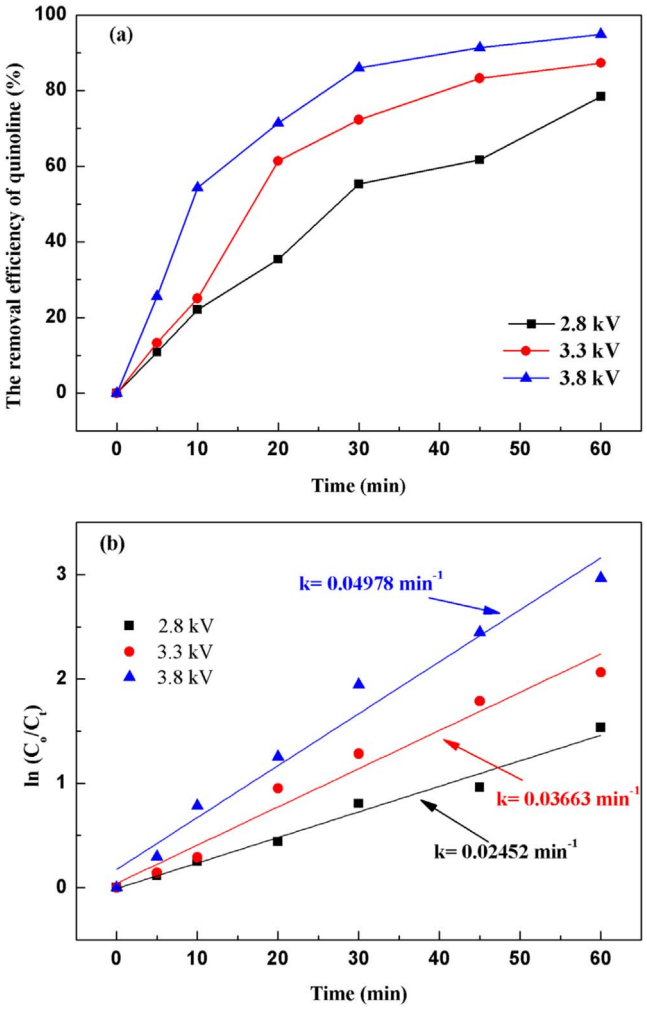

Figure 4. Effect of the input voltage on quinoline degradation: (a) removal efficiency, (b) kinetic constant.

3.2.2. Effect of initial pH value on degradation of quinoline. To investigate the influence of initial pH value during strong ionization discharge, three different initial pH values were selected: pH 5.3 (acid), pH 7.2 (natural pH) and pH 10.1 (alkaline). Under experimental conditions, the input voltage was 3.8 kV, the frequency was 15 kHz, the initial concentration of quinoline was 20 mg l^{-1} and the treated water was 40 l in sample tank. The removal efficiencies of each water sample for different treatment times and different pH are summarized in figure 5(a). As shown in figure 5(a), when pH values were 5.3, 7.2 and 10.1, the removal efficiencies of quinoline after 60 min treatment were 86.2%, 94.8% and 81.6%, respectively, under the same conditions. Analogously, greater kinetic constant can be obtained at natural pH (7.2), as shown in figure 5(b), showing that pH value has little effect on the degradation efficiency of quinoline. Quinoline has a better degradation

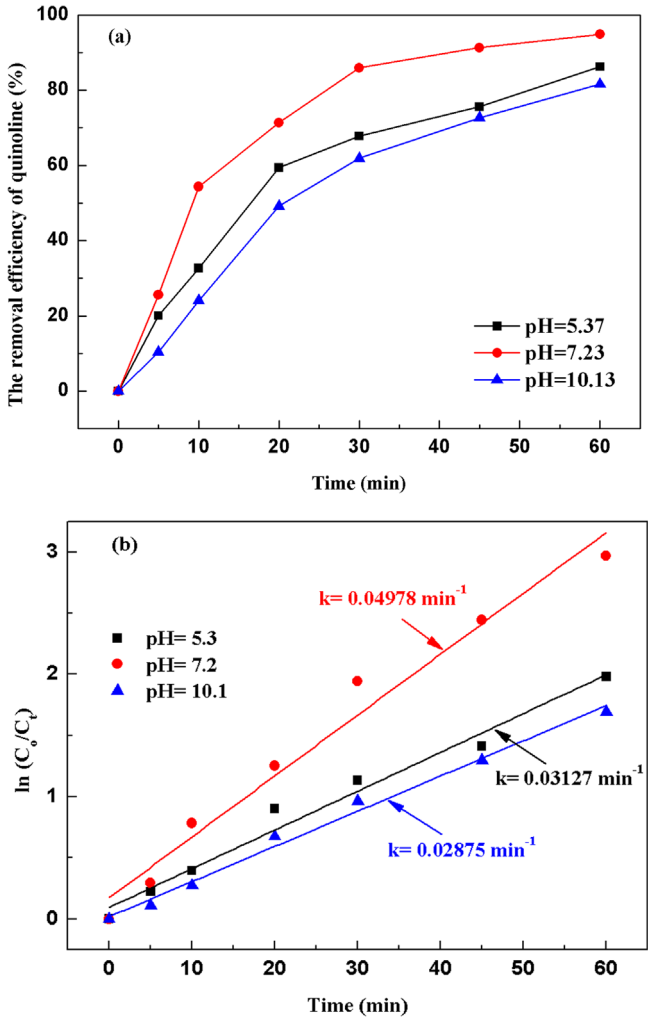

Figure 5. Effect of the initial pH value on quinoline degradation: (a) removal efficiency, (b) kinetic constant.

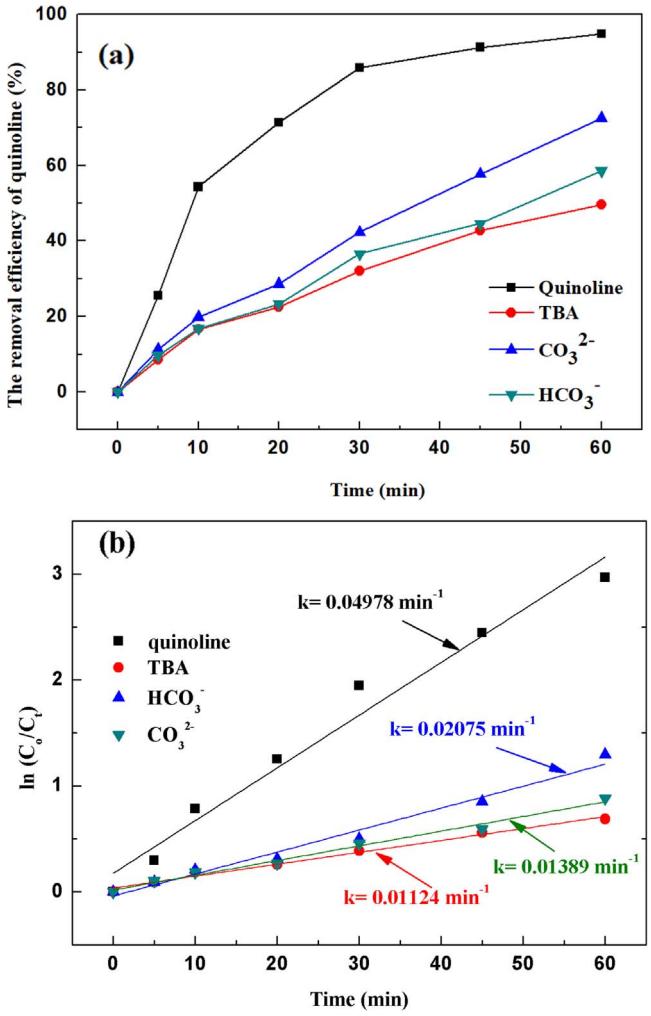

Figure 6. Effect of the ·OH inhibitors on quinoline degradation: (a) removal efficiency, (b) kinetic constant.

effect under neutral conditions, which is better under alkaline conditions than that under acidic conditions that could be explained by the higher stability but lower solubility of O_3 under acidic conditions [36]. It is well known that the solubility of O_3 in acidic solution is higher than that in alkaline solution. Therefore, ozonation in acidic solution plays a key role in improving the degradation efficiency of organic compounds. Under alkaline conditions, ·OH promoted the decomposition of O_3 and generate ·OH with stronger oxidizing properties [37] (R10)–(R12). Thus, the active particles degraded quinoline faster under alkaline conditions. However, the generation rate of ·OH was accelerated, and the decomposition rate was also accelerated, and the reaction time with organic substances was shortened. Meanwhile, the redox potentials of ·OH and O_3 decreased with the increase of pH. When pH changed from 3 to 9, the redox potential of ·OH changed from 2.7 to 2.3 V, reducing the reaction rate [38]. As a result, the strong ionization discharge DBD system is suitable for both acidic solution pollutants and alkaline solution pollutants. In fact, in real engineering applications, in order to utilize the degradation advantages of strong ionization DBD reaction system better, pH value of the influent water quality can be adjusted under neutral conditions, to achieve the maximum degradation efficiency of DBD.

$$OH^- + O_3 \rightarrow O_2^- + HO_2\cdot \quad \text{(R10)}$$

$$HO_2\cdot + O_3 \rightarrow \cdot OH + 2O_2 \quad \text{(R11)}$$

$$OH^- + \cdot OH \rightarrow O\cdot^- + H_2O. \quad \text{(R12)}$$

3.2.3. Effect of hydroxyl radical inhibitors in solution on degradation of quinoline. It has been verified above that both ·OH and O_3 can be formed in the strong ionization discharge DBD system, but the presence of different inhibitors in the solution on the degradation of quinoline by strong ionization discharge needs to be studied. As shown in figure 6(a), with *tert*-butyl alcohol (TBA), CO_3^{2-} and HCO_3^- concentration increased from 0 mg l^{-1} to 30 mg l^{-1}, the removal efficiency of quinoline decreased from 94.8% to 49.6%, 72.5% and 58.5%, respectively, within 60 min strong ionization discharge DBD oxidation process. The kinetic constant decreased from 0.055 min^{-1} to 0.0167 min^{-1}, 0.0216 min^{-1} and 0.0767 min^{-1} in strong ionization discharge DBD system with TBA, CO_3^{2-} and HCO_3^-,

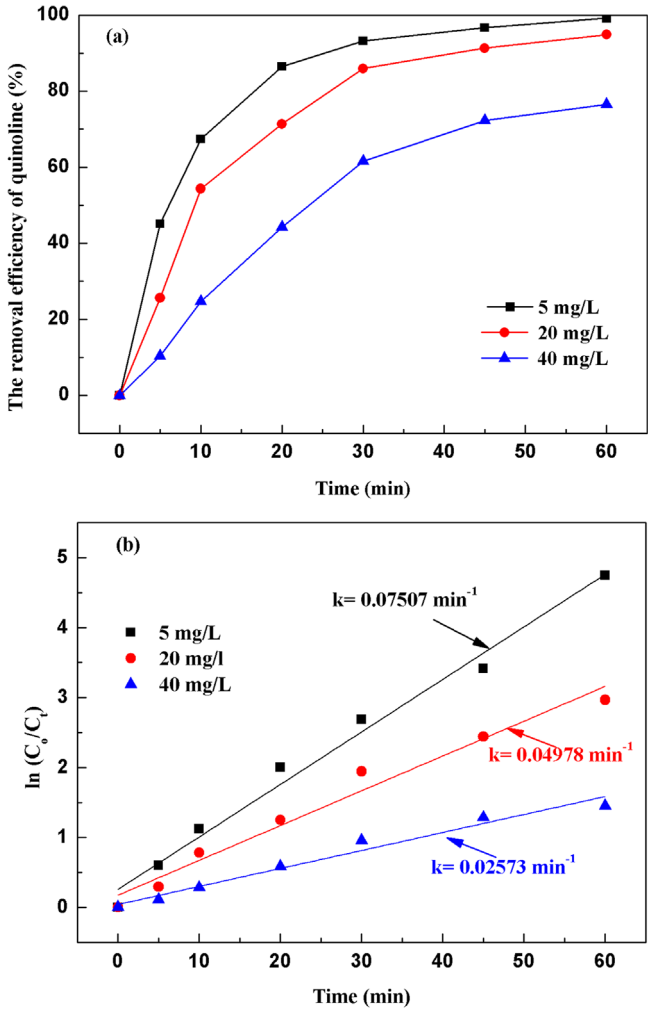

Figure 7. Effect of the initial concentration on quinoline degradation: (a) removal efficiency, (b) kinetic constant.

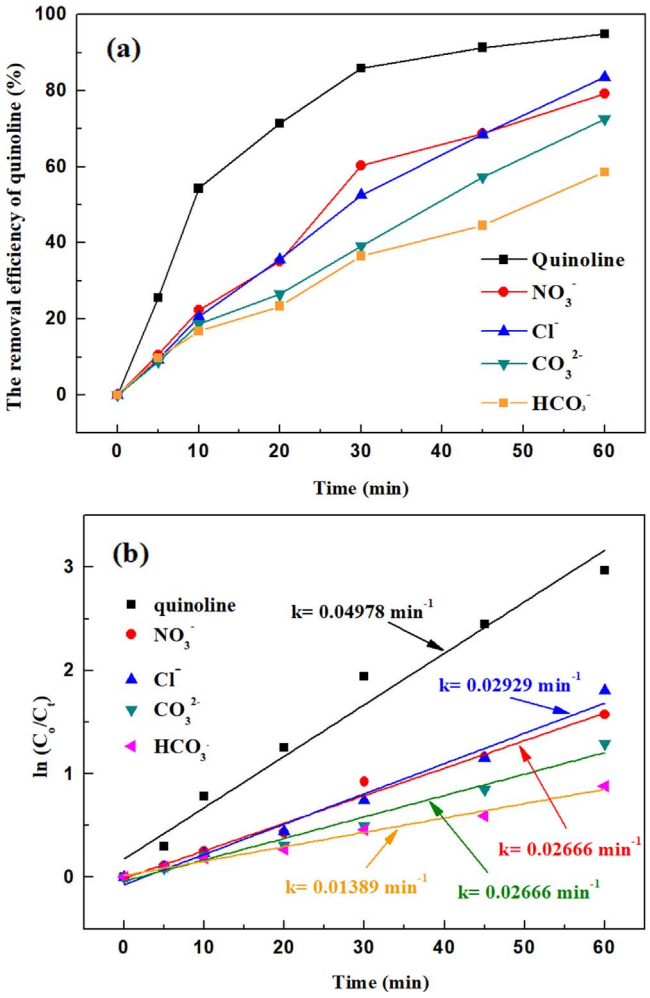

Figure 8. Effect of the inorganic ions on quinoline degradation: (a) removal efficiency, (b) kinetic constant.

respectively (figure 6(b)). The results showed that the degradation of quinoline was substantially inhibited by the addition of inhibitors TBA, CO_3^{2-} and HCO_3^-, which could inhibit the formation of ·OH in the active particles, and ·OH should be responsible for the rapid degradation of quinoline, and it can be implied that alcohols with no α-hydrogen (TBA) are more effective in quenching ·OH than CO_3^{2-} and HCO_3^- [39].

3.2.4. Effect of initial concentration on degradation of quinoline. With a fixed input voltage (3.8 kV), discharge frequency (15 kHz) and pH value (7.2), the effect of the initial concentration on degradation of quinoline was investigated and depicted in figure 7(a). As illustrated in figure 7(a), after 60 min strong ionization discharge treatment, the removal efficiencies of quinoline accordingly decreased with the increase of initial quinoline concentration from 5 mg l^{-1} to 40 mg l^{-1}, with the degradation rates of quinoline of 99.1%, 94.8% and 80.5%, respectively. Similarly, figure 7(b) showed that the kinetic constant can be decreased when the initial concentrations on quinoline were increased, which can vary from 0.055 min^{-1} to 0.045 min^{-1}, 0.036 min^{-1}, 0.025 min^{-1}.

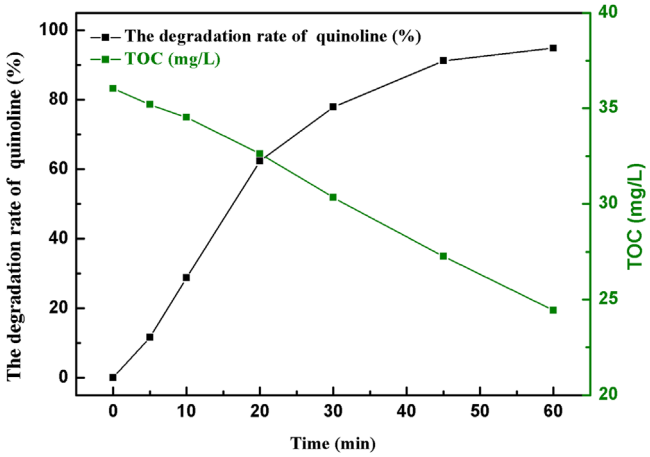

Figure 9. The degradation efficiency of quinoline and TOC removal.

Due to the higher initial solution concentration, the active particles produced by the strongly ionized discharge were more and more consumed, which further confirmed that strong ionization discharge in the treatment of high concentrations of contaminants in the water will be a

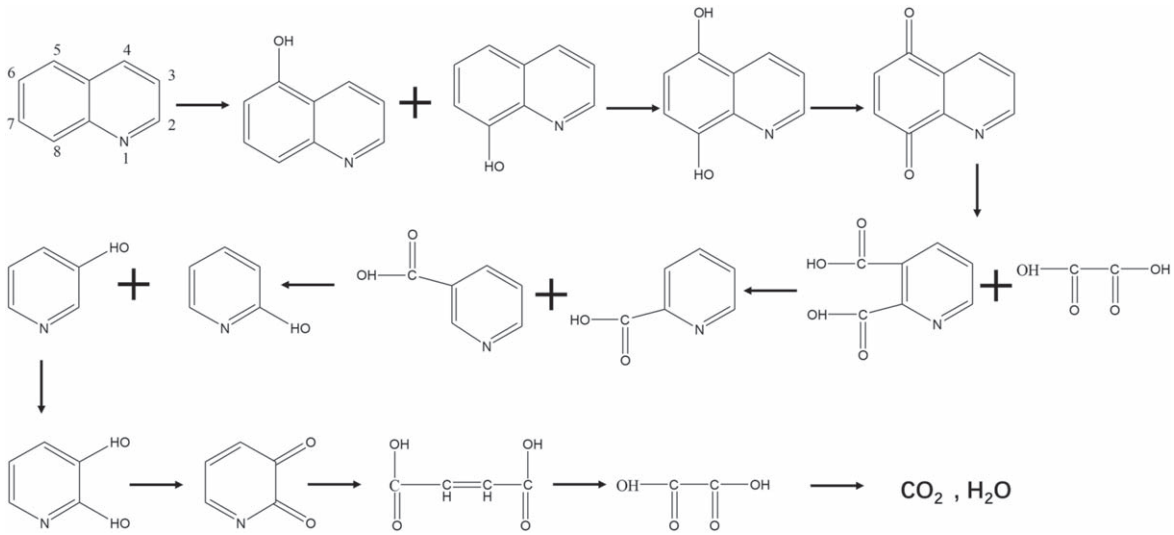

Figure 10. Proposed reaction pathway for the degradation of quinoline by a strong ionization discharge DBD.

greater impact. Therefore, the development of high power for different water quality of the strong ionization barrier discharge equipment in the promotion of industry has a very important significance.

3.2.5. Effect of inorganic ions in water on the degradation of quinoline. Inorganic ions are common in all kinds of water, inorganic ions are an important indicator to study the water physical and chemical factors on the degradation of pollutants [40]. With a fixed input voltage (3.8 kV), discharge frequency (15 kHz) and pH value (7.2), the concentrations of inorganic ions such as NO_3^-, Cl^-, CO_3^{2-} and HCO_3^- were added to the water to 30 mg l^{-1} respectively. The effect of inorganic ions on the removal efficiency of quinoline was investigated by analyzing the water samples at different times. As illustrated in figure 8(a), the removal efficiencies of quinoline were 83.5% and 79.2%, respectively, after 30 mg l^{-1} Cl^- and NO_3^- were added to the water sample before treatment. Under the same conditions with the addition of CO_3^{2-} and HCO_3^-, the removal efficiencies of quinoline were 72.5% and 58.5%, respectively. The removal efficiency of CO_3^{2-} and HCO_3^- quinoline was weaker than the removal efficiency of NO_3^-, Cl^-, which can be attributed to their inhibition with ·OH. The two ions are ·OH inhibitors, to some extent, inhibited the indirect oxidation of O_3 and ·OH generation, resulting in the degradation of quinoline in water mainly through direct oxidation of O_3. Figure 8(b) suggests that the highest kinetic constant was 0.045 with NO_3^-, whereas 0.034 min^{-1}, 0.028 min^{-1} and 0.038 min^{-1} can be obtained with CO_3^{2-}, HCO_3^- and Cl^-, respectively. Among the examined four kinds of inorganic ions, the solutions with Cl^- and NO_3^- were relatively more easily removed, while CO_3^{2-} and HCO_3^- have a great influence on the removal efficiency of quinoline, especially HCO_3^-. Therefore, in practical application, when the water contains a high content of CO_3^{2-} and HCO_3^-, certain pretreatment should be first carried out, such as adjusting the water quality to acid or adding lime milk and other types of ions to remove.

3.3. Possible degradation mechanism of quinoline

Input voltages, initial pH value, initial concentration, radical inhibitors and inorganic ions all had significant effects on degradation of quinoline. The optimal experimental conditions were 3.8 kV, 15 kHz, with initial concentration of quinoline of 20 mg l^{-1}, ·OH concentration of 0.74 mmol l^{-1} and O_3 concentration of 58.2 mg l^{-1}. As presented in figure 9, after 60 min of a strong ionization discharge DBD treatment, the removal efficiency of quinoline accordingly increased up to 94.8%. From the comparison of the degradation kinetic constant of quinoline by O_3 alone (0.0053 min^{-1}), O_3/UV (0.0304 min^{-1}) and O_3/photocatalytic (0.0056–0.0278 min^{-1}) [2, 41, 42], it was found that the kinetic constant of quinoline in strong ionization discharge DBD system was more fast (0.050 min^{-1}). At the same time, the TOC decreased from 36.0 to 24.4 mg l^{-1}. To clarify the degradation mechanism to the removal of quinoline by a strong ionization discharge DBD treatment, the water samples with different treatment time (5 min, 10 min, 30 min, 60 min) were detected by LC–MS.

Quinoline is composed of two aromatic rings, one benzene ring and one pyridine ring. According to the electron cloud distribution of quinoline in figure A2, the electron cloud density on the benzene ring is higher than that on the pyridine ring [3], so the electrophilic reaction of active ions mainly occurs on the benzene ring with high electron cloud density. Therefore, the electrophilic reaction of quinoline oxidation mainly focused on the fifth and eighth sites [1]. O_3 and ·OH are electrophiles that react with quinoline. Previous studies have reported that the oxidation reaction of quinoline with strong oxidant is mainly to break the benzene ring and form pyridine 2, 3-dicarboxylate [41].

Therefore, the strong ionization DBD reaction system was used to produce active particles to degrade quinoline in drinking water. The first step of quinoline oxidation was

hydroxyl dehydrogenation. The active particles mainly attacked the fifth and eighth positions of quinoline to form hydroxyquinoline. Similarly, dihydroxyquinoline (5-hydroxy quinoline or 8-hydroxyquinoline) was produced to continuously process the above reaction. The hydroxyl group can be oxidized to the acyl group, and then to a carboxyl group. Then, the ring-opening reaction occurred in benzene ring, oxalic acid and pyridine 2,3-dicarboxylate are formed. Dehydrogenation of hydroxyl radicals resulted in decarboxylation of pyridine dicarboxylic acid, thus removing one carboxyl group to form pyridine 2-formate or pyridine 3-formate. Moreover, heterocyclic base compounds had certain alkalinity and had the catalytic action similar to homogeneous base. Therefore, quinoline could promote the ionization of carboxylic acid, thus increasing the ion concentration of carboxylic acid and accelerating the decarboxylation reaction. Specifically, the formation of hydroxypyridine was the decarboxylation of pyridine formate, which replaces the existing carboxyl group with the hydroxyl group. In addition, the hydroxyl group in hydroxy pyridine was oxidized to form an acyl group, which opens the pyridine ring and then produces substances such as fumaric acid. As far as macromolecular acids are concerned, they were finally oxidized into small molecular acids such as oxalic acid, formic acid, etc, and then mineralized into CO_2 and water. In general, the possible pathways for the degradation of quinoline were reflected in figure 10, while the mass spectrum as well as the proposed fragmentation pattern of reaction byproduct were dipicted in figures A3–A13.

3.4. Residual toxicity analysis of byproducts

It is necessary to consider the toxicity of byproducts in the DBD process. According to the Toxicity Estimation Software Tool (T.E.S.T.) analysis, figure 11 predicted the changes in the acute toxicity, bioaccumulation factor, and mutagenicity of these intermediates. Among all intermediate byproducts, only the oral rat LD50 of m/z 157 could not be calculated. As displayed in figure 11(a), the oral rat LD50 of m/z 168, m/z 96 (a), m/z 96 (b), and m/z 90 were 1002.72 mg kg^{-1}, 426.6 mg kg^{-1}, 426.6 mg kg^{-1} and 534.39 mg kg^{-1}, respectively, which were more toxicity than quinoline and supposed to 'very toxicity'. Although m/z 161, m/z 157, and m/z 112 were supposed to 'toxic' in figure 11(b), the final intermediates were mainly m/z 145 (b), m/z 124 (b), m/z 96 (a), and m/z 90, and the acute toxicity of LC50 (Daphnia magna LC50 (96 h)) of these byproducts was lower than that of quinoline. It is exciting that the mutagenicity of most quinoline byproducts was reduced into 'mutagenicity negative'. Similarly, the values of bioaccumulation factors of these intermediates were increased compared with the original quinoline solution. The bioaccumulation factor of quinoline was 95.14, m/z 168, m/z 124, m/z 116, and m/z 90 decreased by 99.84%, 99.14%, 99.36%, and 99.82%, respectively, referring to quinoline. The results showed clearly that, in terms of the oral rat LD50, Daphnia magna LC50 (96 h), mutagenicity and bioaccumulation factor, although DBD treatment cannot completely degrade quinoline to non-toxicity, it did alleviate the toxicity of quinoline by converting it into intermediate byproducts.

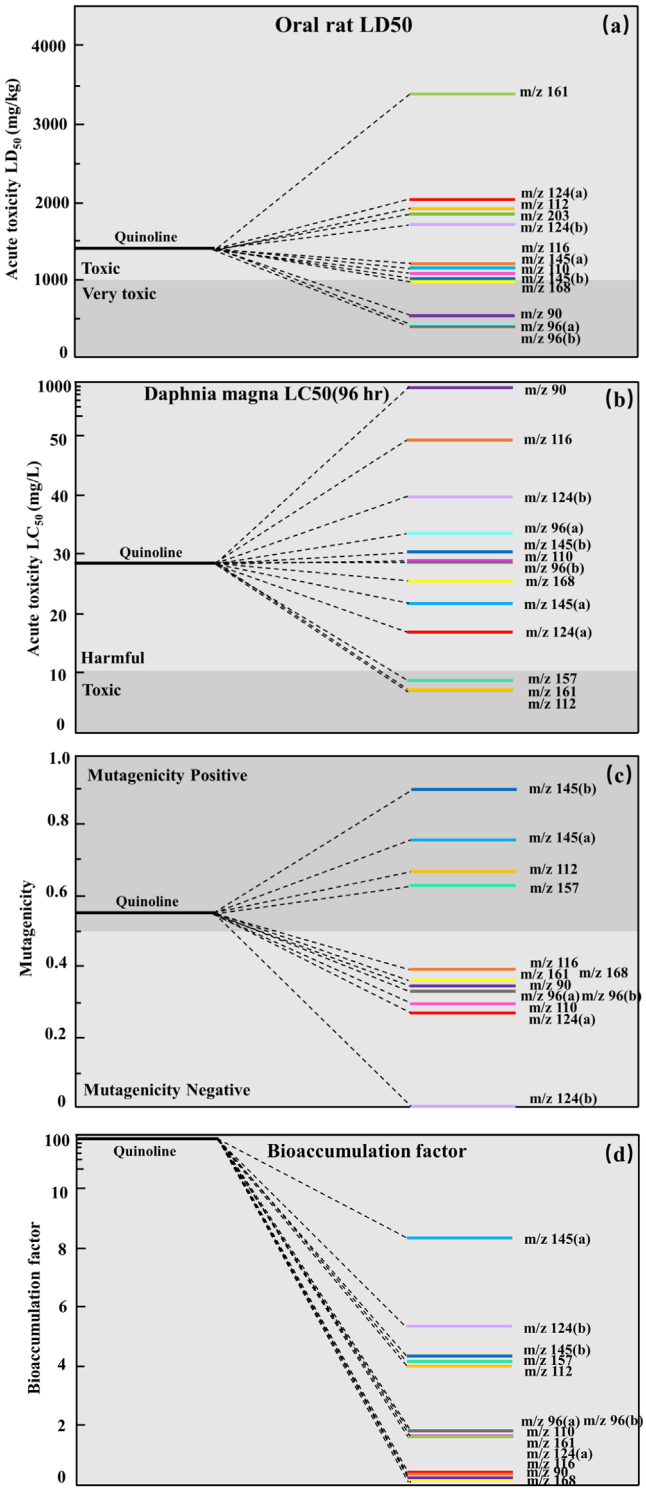

Figure 11. Residual toxicity of the quinoline solution after treatment: (a) oral rat LD50, (b) daphnia magna LC50, (c) mutagenicity, (d) bioaccumulation factor.

4. Conclusions

The degradation performance of quinoline by a new large volume DBD water treatment system was studied. Current results proved that a strong ionization discharge DBD reactor can produce a high concentration of ·OH and O_3, which can

remove quinoline effectively. The results of ESR and O_3 analysis show that ·OH and O_3 generated by strong ionization DBD played major roles during the oxidation. The enhanced quinoline abatement efficiency at different input voltages, initial pH value, initial concentration and inorganic ions was explored. With the increase of the input voltage and the decrease of initial concentration, the removal efficiency and the kinetic constant of quinoline increased gradually, and the increasing trend was obvious. The effect of pH value on the removal efficiency and the kinetic constant of quinoline was not obvious, indicating that the performance of quinoline was better under neutral conditions, and the removal efficiency of quinoline was higher than that under acidic conditions. The oxidation of quinoline by Cl^- and NO_3^- ions in inorganic ions had less effect on removal quinoline, but CO_3^{2-} and HCO_3^- had a great influence on the degradation of quinoline, which greatly reduced the removal efficiency of quinoline. A possible degradation pathway of quinoline was through hydroxyl dehydrogenation and decarboxylation reaction step-by-step and was determined by LC–MS analysis. Moreover, the toxicity analysis of byproducts showed that the toxicity at the oral rat LD50, daphnia magna LC50 (96 h), mutagenicity and the bioaccumulation factor was reduced. Therefore, a strong ionization DBD technology could provide new insight into quinoline wastewater treatment.

Acknowledgments

Thanks to National Natural Science Foundation of China (No. 32071521), the Postgraduate Research & Practice Innovation Program of Jiangsu Province (No. KYCX18_2272), the Priority Academic Program Development of Jiangsu Higher Education Institutions (PAPD) and Jiangsu Collaborative Innovation Center of Technology and Material of Water Treatment for their support of this work.

Appendix

Table A1. Methods of LC–MS instrument conditions for quinoline.

Time (min)	Gradient program	The mobile phase	
0	100% A, 0% B	A (95% water, 5% methanol, and 0.1% formic acid) and B (5% water, 95% methanol, and 0.1% formic acid)	
1	50% A, 50% B	Flow rate	0.3 l min^{-1}
10	50% A, 50% B	Injection volume	5 μl
11.5	10% A, 90% B	Gas temperature	300 °C
11.6	100% A, 0% B	Ionization	Positive ion
15	100% A, 0% B	Source voltage	3.5 kV
0	100% A, 0% B		

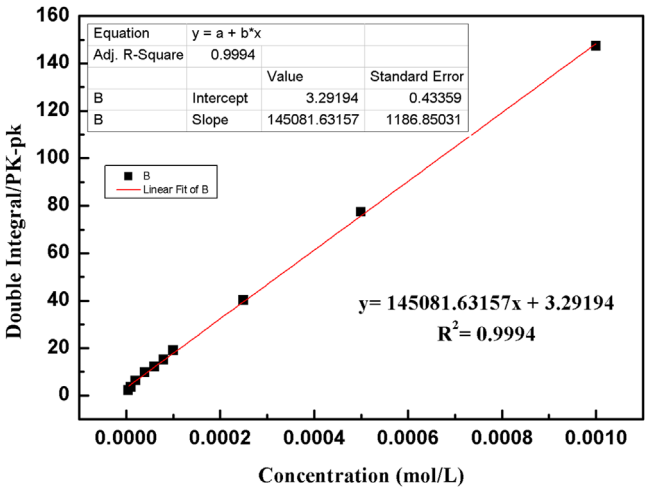

Figure A1. Standard curve of ·OH concentration.

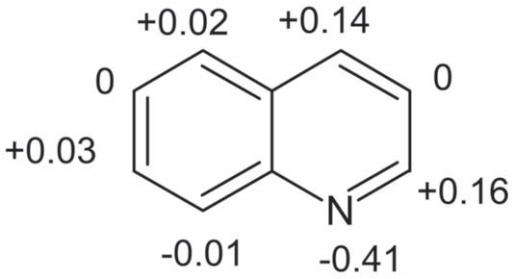

Figure A2. The electron cloud distribution of quinoline.

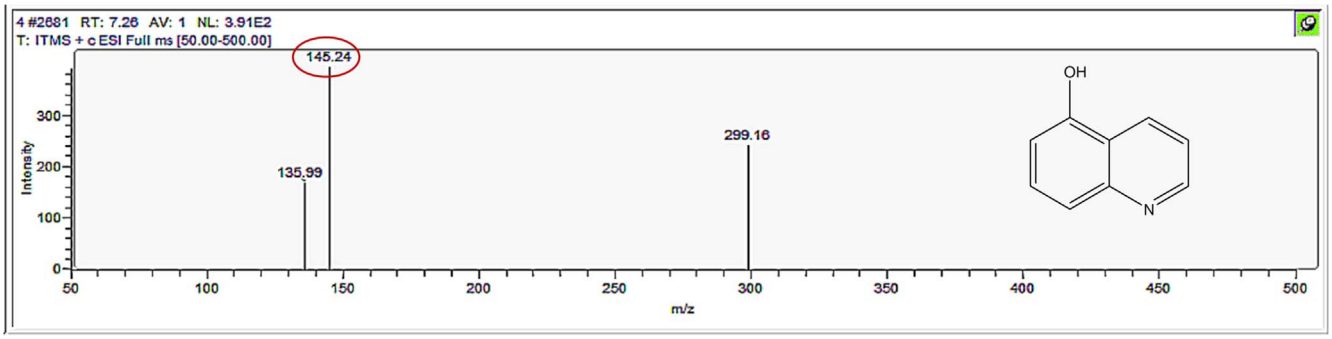

Figure A3. Mass spectrum and proposed fragmentation pattern of reaction byproduct with m/z 145(a).

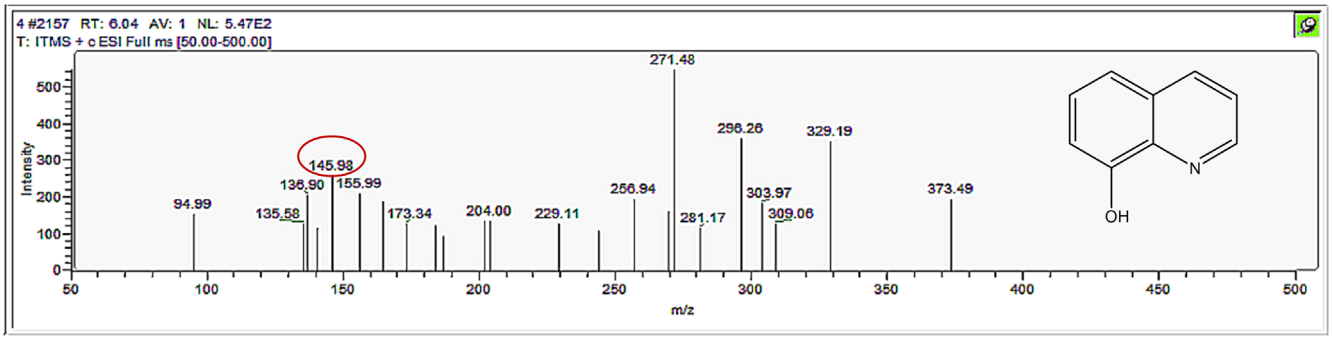

Figure A4. Mass spectrum and proposed fragmentation pattern of reaction byproduct with m/z 145(b).

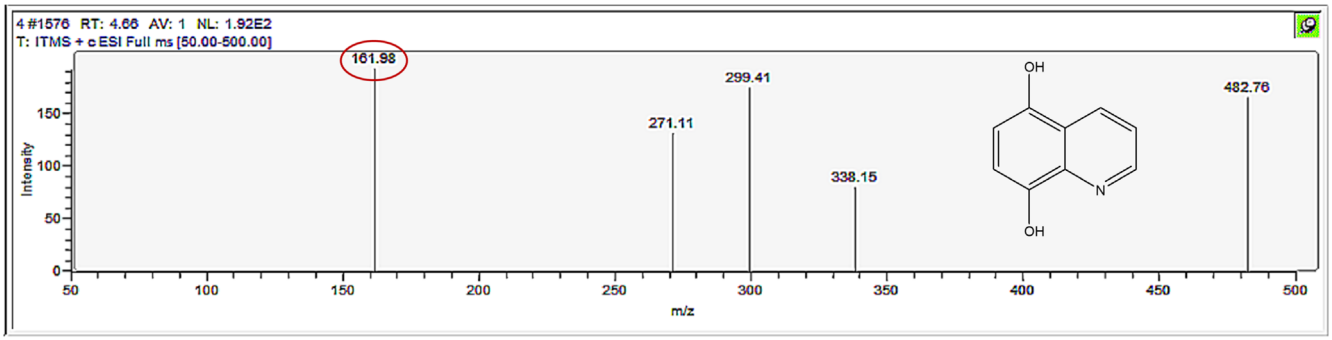

Figure A5. Mass spectrum and proposed fragmentation pattern of reaction byproduct with m/z 161.

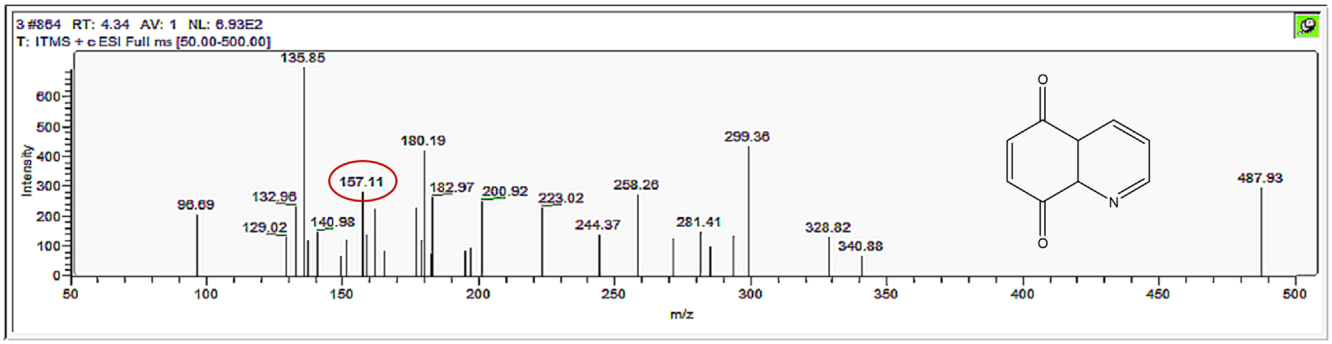

Figure A6. Mass spectrum and proposed fragmentation pattern of reaction byproduct with m/z 157.

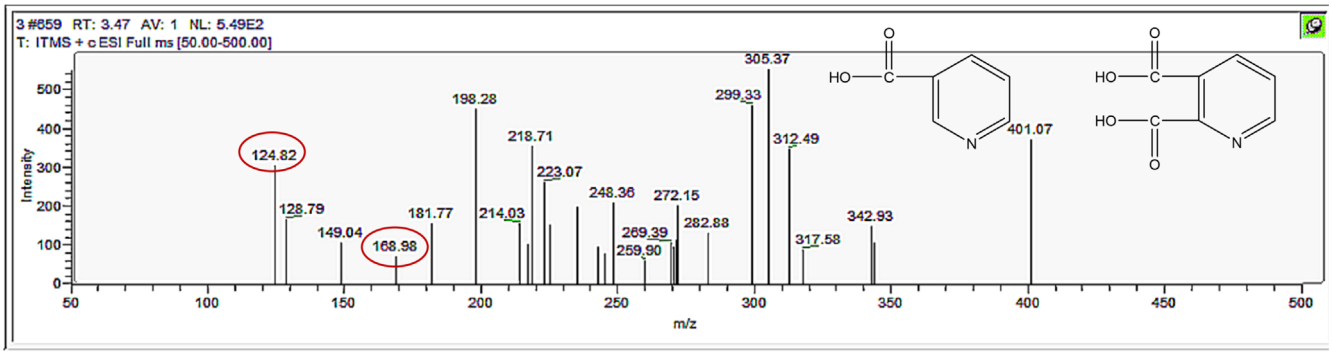

Figure A7. Mass spectrum and proposed fragmentation pattern of reaction byproduct with m/z 168 and m/z 124.

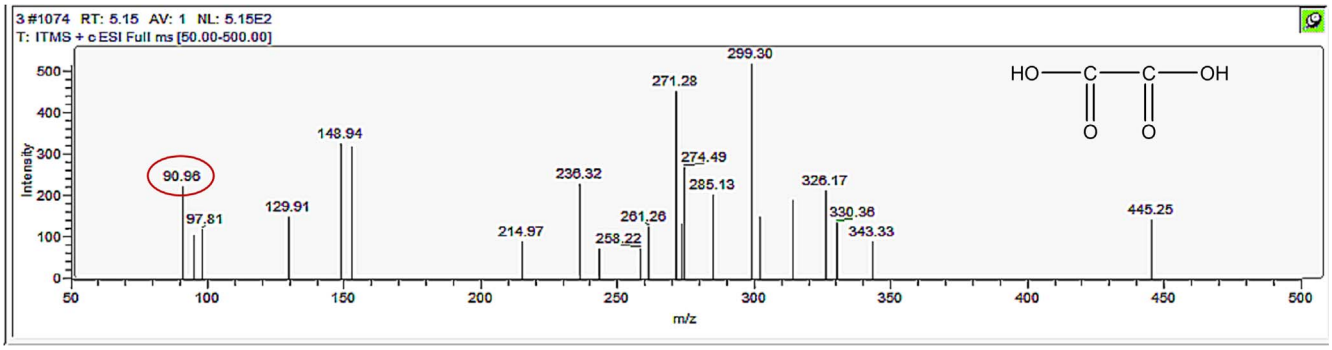

Figure A8. Mass spectrum and proposed fragmentation pattern of reaction byproduct with m/z 90.

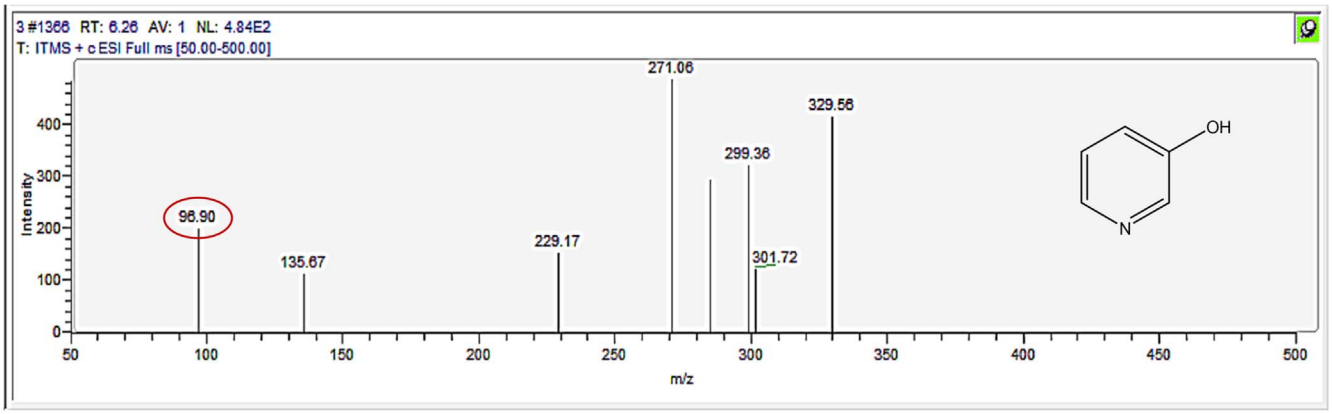

Figure A9. Mass spectrum and proposed fragmentation pattern of reaction byproduct with m/z 96(a).

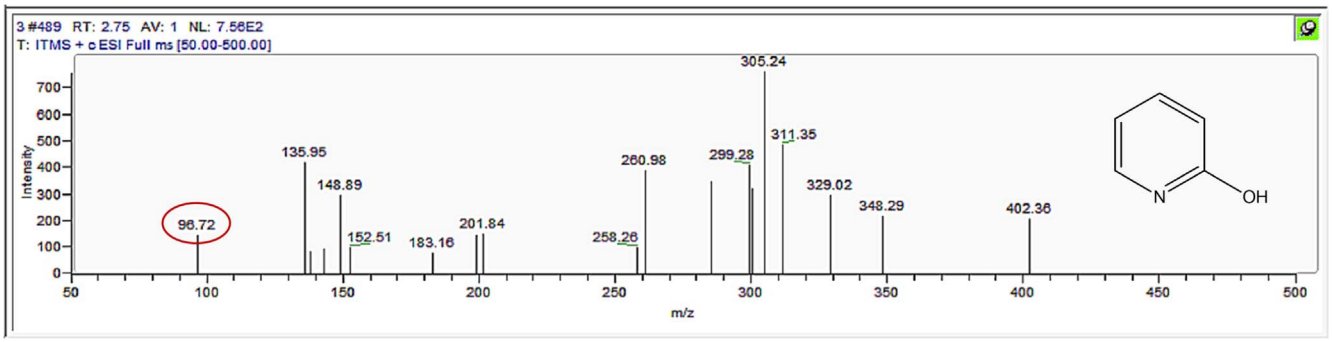

Figure A10. Mass spectrum and proposed fragmentation pattern of reaction byproduct with m/z 96(b).

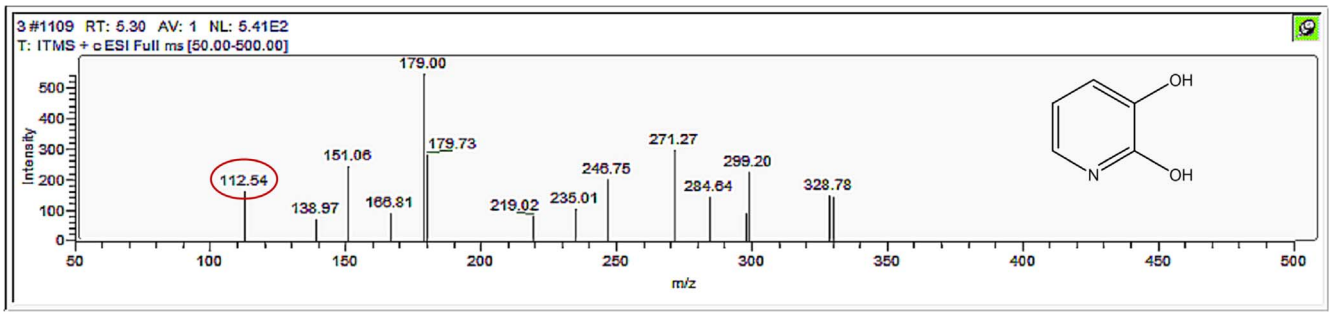

Figure A11. Mass spectrum and proposed fragmentation pattern of reaction byproduct with m/z 112.

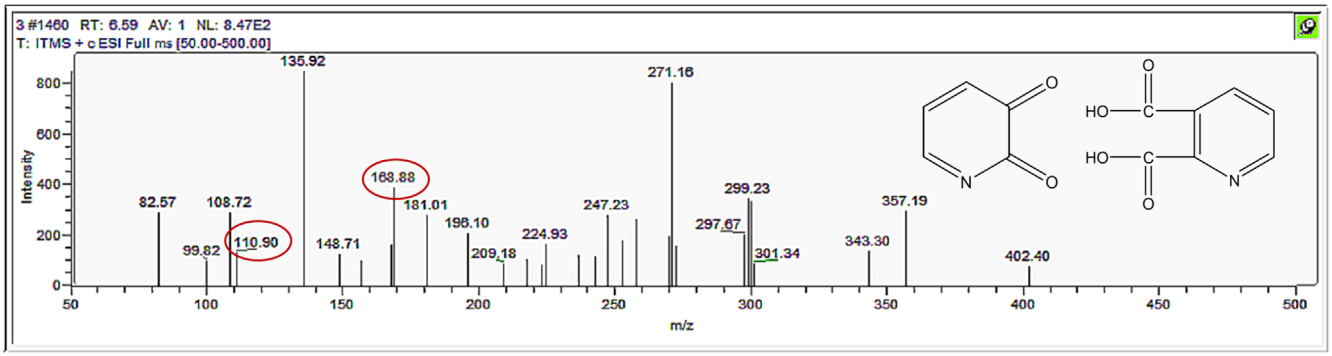

Figure A12. Mass spectrum and proposed fragmentation pattern of reaction byproduct with m/z 110 and m/z 168.

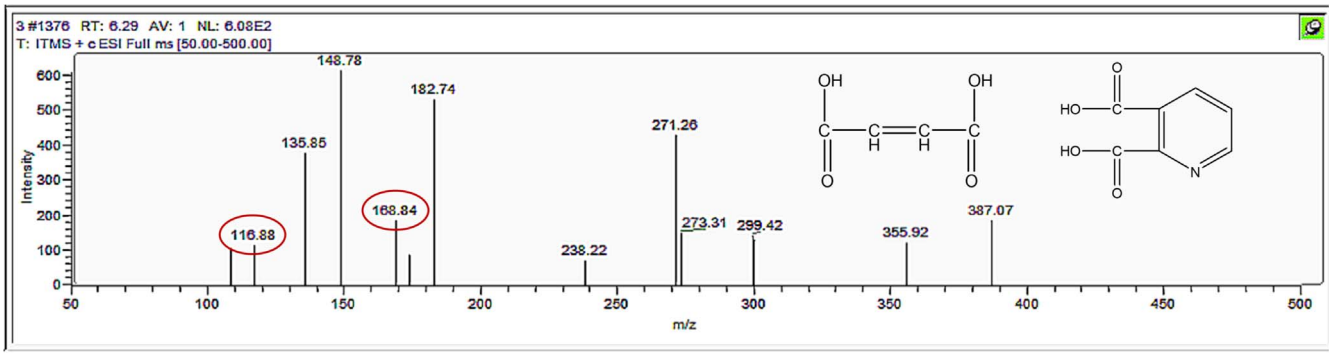

Figure A13. Mass spectrum and proposed fragmentation pattern of reaction byproduct with m/z 116 and m/z 168.

Table A2. Methods of ESR instrument conditions for quinoline.

Resonance frequency	9.77 GHz	Microwave power	19.97 mW
Sweep width	100 G	Time constant	40.96 ms
Receiver gain	1.0×10^4	Modulation amplitude	1.0 G
Weep time	83.89 s		

Table A3. Discharge parameters and energy consumption of strong ionization.

Voltage (kV)	Electric current (mA)	Power (W)	Frequency (kHz)	Energy consumption (kWh)	Power consumption (kJ/(mg l^{-1}))
2.8	81.07	234.57	16.47	0.082	21.61
3.3	136.75	441.77	13.03	0.154	28.76
3.8	156.5	559.63	17.89	0.195	34.07

Table A4. Organic wastewater treatment methods and its energy consumption.

Source	Methods	Energy consumption (kWh m^{-3})
Organic wastewater (dye, medicine, pesticide, etc)	Sedimentation-activated sludge-dewatering	1.85–0.95
	Contact oxidation process	2.4–1.35
	chemical oxidation	1.35–0.7
	Incineration	23.8
	O_3 only	13.35
	US/O_3	30.34
	O_3/EC	7.8
	US/O_3//EC	8
	pre ozonation/biological	57.43
	post-ozonation/biological	51.41
	Strong ionization discharge	0.133

References

[1] Wang C R *et al* 2016 *Chemosphere* **149** 219
[2] Liu D *et al* 2019 *Chemosphere* **227** 647
[3] Jing J Y *et al* 2012 *J. Hazard. Mater.* **237–238** 247
[4] Li Y M *et al* 2010 *J. Hazard. Mater.* **173** 151
[5] Rameshraja D *et al* 2018 *Chem. Pap.* **72** 617
[6] Pachupate N J and Vaidya P D 2018 *J. Environ. Chem. Eng.* **6** 883
[7] Bai Q *et al* 2015 *Environ. Sci. Technol.* **49** 11536
[8] Qiao L and Wang J L 2010 *Bioresour. Technol.* **101** 7683
[9] Lee M *et al* 2017 *Environ. Sci. Technol.* **51** 497
[10] Wang Z X 2014 *MSc Thesis* Dalian University of Technology (in Chinese) (https://kns.cnki.net/KCMS/detail/detail.aspx?dbname=CDFDLAST2015&filename=1015571933.nh)
[11] Moreira N F F *et al* 2015 *Water Res.* **87** 87
[12] Gümüş D and Akbal F 2017 *Chemosphere* **174** 218
[13] Guo H *et al* 2021 *Sep. Purif. Technol.* **266** 118543
[14] Zhang Z T *et al* 2002 *Poll. Cont.* **3** 25
[15] Guo H *et al* 2021 *J. Hazard. Mater.* **403** 123673
[16] Li R J *et al* 2021 *Sep. Purif. Technol.* **274** 119103
[17] Wang B W *et al* 2017 *J. Adv. Oxid. Technol.* **20** 196
[18] Iervolino G, Vaiano V and Palma V 2019 *Sep. Purif. Technol.* **215** 155
[19] Guo H *et al* 2021 *Chemosphere* https://doi.org/10.1016/j.chemosphere.2021.131156)
[20] Gao L H *et al* 2013 *Chem. Eng. J.* **228** 790
[21] Marotta E *et al* 2011 *Plasma Process. Polym.* **8** 867
[22] Wang J *et al* 2020 *Chem. Eng. J.* **390** 124512
[23] Guo H *et al* 2021 *Vacuum* **185** 110022
[24] Bai M D *et al* 2005 *Plasma Chem. Plasma Process.* **25** 539
[25] Zhang Y B *et al* 2013 *Plasma Chem. Plasma Process.* **33** 751
[26] Tao X M *et al* 2011 *Prog. Energy Combust. Sci.* **37** 113
[27] Napartovich A P 2001 *Plasmas Polym.* **6** 1
[28] Fridman A, Chirokov A and Gutsol A 2005 *J. Phys. D.: Appl. Phys.* **38** R1
[29] Miao H and Yun G 2011 *Appl. Surf. Sci.* **257** 7065
[30] Esposito E X *et al* 2005 *Methods Mol. Biol.* **275** 131
[31] Hijosa-Valsero M *et al* 2013 *J. Hazard. Mater.* **262** 664
[32] Asaithambi P *et al* 2020 *Process. Saf. Environ. Prot.* **142** 212
[33] He C C *et al* 2016 *Sep. Purif. Technol.* **165** 107
[34] Bilińska L *et al* 2019 *Chem. Eng. J.* **358** 992
[35] Irani R *et al* 2020 *J. Environ. Chem. Eng.* **9** 104595
[36] Oulton R *et al* 2015 *Environ. Sci. Technol.* **49** 3687
[37] Wu J L *et al* 2020 *Chem. Eng. J.* **384** 123300
[38] Guo H *et al* 2018 *Chem. Eng. J.* **425** 130614
[39] Bao Y P *et al* 2019 *Appl. Catal.* B **254** 37
[40] Bing J S *et al* 2015 *Environ. Sci. Technol.* **49** 1690
[41] Wang X M *et al* 2004 *Chemosphere* **55** 733
[42] Gupta D *et al* 2020 *J. Environ. Manage.* **258** 110032